Microwave resonance studies on $Tm^{3+}(4f^{12})$ diluted into single-crystal monoclinic $YCl_3 \cdot 6H_2O$ and $Y_2(SO_4)_3 \cdot 8H_2O$†

Ivan E. Rouse
Department of Physical Sciences, Union College, Lincoln, Nebraska 68506

John B. Gruber
College of Science and Mathematics, Department of Physics, North Dakota State University, Fargo, North Dakota 58102

(Received 14 July 1975)

Both electric-dipole and magnetic-dipole microwave transitions have been observed between the ground and first excited nondegenerate Stark levels of $Tm^{3+}(4f^{12})$ doped into diamagnetic monoclinic $YCl_3 \cdot 6H_2O$ and $Y_2(SO_4)_3 \cdot 8H_2O$. The zero magnetic field separation between levels, Δ, is small enough (1 cm^{-1}) that microwave data can be collected using both K-band (~ 24 GHz) and K_a-band (~ 35 GHz) spectrometers. Experiments were carried out at approximately 1.5°K. Orientation-dependence measurements were made of line positions, relative line intensities, linewidths, and line shapes. In many cases the angular dependence agrees with that predicted. However, at large angles between $g_{\parallel}\cos\alpha$ and the magnetic field we observed splitting of the hyperfine lines which we cannot explain. Values of Δ, $g_{\parallel}\cos\alpha$, $A_{\parallel}/\cos\alpha$, and $G_{\perp}$ (the "electric" g value) are reported. The magnitude of $G_{\perp}$, 115 ± 35 cgs units, is very large in comparison to values reported for other rare-earth ions in similar salts, but can be understood in terms of the experimental values of Δ and $g_{\parallel}\cos\alpha$ reported.

I. INTRODUCTION

Recent optical-absorption, Zeeman, and magnetic resonance studies[1-8] have revealed a small energy separation between the nondegenerate ground and first excited Stark levels of the ground state $^3H_6$ of Tm^{3+} in monoclinic single crystals of $Tm_2(SO_4)_3 \cdot 8H_2O$, $TmCl_3 \cdot 6H_2O$, and Tm^{3+} doped into $Y_2(SO_4)_3 \cdot 8H_2O$ and $YCl_3 \cdot 6H_2O$. Because the site symmetry of the thulium ion is so low in these crystals, the $2J+1$ degeneracy associated with each J manifold of Tm^{3+} is completely lifted by the action of the crystalline electric field (CEF). The point-group symmetry for Tm^{3+} in the hydrated chloride salts is reported as C_2 by Marezio, Plettinger, and Zachariasen.[9] The point-group symmetry for Tm^{3+} in the hydrated sulfate salts has been deduced to be C_{1h} from recent optical studies.[6,7] The reported optical data including the near accidental degeneracy of the ground state have been interpreted recently in terms of CEF theory and higher symmetry effects.[4-8]

Knowing the point-group symmetry, the CEF wave functions, and the energy separation between levels, it has been possible to predict and observe microwave electric-dipole (ED) as well as microwave magnetic-dipole (MD) transitions in these salts.[10] Further, it has been reported that Tm^{3+} resides in two equally abundant types of magnetically inequivalent sites in the hydrated sulfate,[11] while in the hydrated chloride there appears to be only one.[2] Yet there exists only one type of crystallographic rare-earth site in each salt.[7,9]

We have recently extended earlier work reported by our group.[1] The present study includes orientation-dependence measurements, relative intensities, linewidths, and line shapes, and includes experimental values for $g_{\parallel}\cos\alpha$, Δ, and $A_{\parallel}/\cos\alpha$. These terms are defined in the following sections.

II. EXPERIMENTAL DETAILS

Single crystals were grown by Karlow of our group, by Dr. U. Wagner, Physics Dept., Technical University, Munich, Germany, and by one of us (I. E. R.). The single crystals contained approximately 0.5% molar concentration of Tm^{3+} substituted into Y^{3+} sites in $Y_2(SO_4)_3 \cdot 8H_2O$ and $YCl_3 \cdot 6H_2O$. The ionic radii for Y^{3+} and Tm^{3+} are nearly the same, being 0.93 and 0.95 Å, respectively, so that Tm^{3+} ions can easily substitute for Y^{3+} ions in the lattice.

Two separate microwave resonance spectrometers were used. For resonance experiments in the frequency range of 34.5–35.5 GHz, we built a spectrometer described by Alger[12] as a reflection homodyne type 3, RH3-Ka, with a balanced mixer. The frequency was measured with a Systron-Donner absorption-type wave meter. Frequency stability was measured to between one part in 4×10^5 and one part in 10^6, with a magnetic field stability of one part in 10^6. Magnetic field measurements were made using a Rawson rotating-coil gaussmeter. Details regarding the spectrometer and its performance are described by one of us[13] (I. E. R.).

The K-band spectrometer, operating in the fre-

quency range around 24 GHz, was assembled by another member of our group (J. E. Bray) using the microwave bridge and klystron power supply from a Strand Labs 602A/K EPR spectrometer with a PAR model HR-8 lock-in amplifier. The accuracy of the wave meter and magnetic field readings was checked against samples of known g values. The experimental g values obtained using this instrument agreed to within four significant figures of the accepted g values.

Cylindrical sample cavities were used with both spectrometers. The cavities were operated either in the TE_{012} or TE_{011} mode. To observe ED transitions, the sample was placed in the cylindrical cavity $0.25L$ from the bottom and $0.5R$ from the cylindrical symmetry axis where the $E_\perp$ microwave field is maximum for the cavity operating in the TE_{012} mode. L and R represent the length and radius of the cavity. To observe MD transitions, the sample was placed on the bottom of the cavity $0.5R$ from the symmetry axis where the $H_\parallel$ microwave field is maximum.

The crystals were mounted in a cylindrical Styrofoam holder using Duco cement with the $g_\parallel$ direction of the sample radial to the symmetry axis of the cavity and thus parallel to the plane of rotation of the external magnetic field. Since it was difficult to position the crystals exactly, we estimate an uncertainty of several percent associated with the $\cos\alpha$ factor which represents a small angle α between $g_\parallel$ and the plane of rotation of the external magnetic field. Observed resonances were studied as the external magnetic field was rotated about the sample. Temperatures near 1.5°K could be achieved by pumping on liquid helium and were read directly from a Wallace-Tiernan pressure gauge.

A. Spin Hamiltonian

For the non-Kramers ion $Tm^{3+}(4f^{12})$ in these salts we can write the following spin Hamiltonian for magnetic and electric dipole microwave transitions between the ground and first excited nondegenerate Stark levels[14,15]:

$$H = g_\parallel \mu_B H_z S_z + A_\parallel I_z S_z + (\Delta_x + G_\perp \mu_B E_x) S_x + (\Delta_y + G_\perp \mu_B E_y) S_y , \quad (1)$$

where $S = \frac{1}{2}$ for a two-level system. Optical-absorption studies[2,7,11] have shown that the higher-energy Stark levels of $^3H_6$ are several hundred wave numbers away, so that the ground and first excited Stark levels separated by about 1 cm^{-1} can be treated as a two-level system at the temperatures reported in our studies (~2°K). In Eq. (1) $g_\parallel = g_z = \langle\psi_2|2\lambda_J J_z|\psi_1\rangle$, and $G_\perp = \langle\psi_2|(\gamma/\mu_B)J_x|\psi_1\rangle$, where γ is a reduced matrix element, μ_B is the Bohr magneton, and ψ_1 and ψ_2 are wave functions for nondegenerate levels 1 and 2 obtained from Refs. 4 and 7. In Eq. (1) $H_z = H\cos\theta$ refers to the component of the applied magnetic field along the $g_\parallel$ direction, E_x and E_y refer to the applied static electric field, and $A_\parallel$ and I_z refer to the nuclear spin of $\frac{1}{2}$ for ^{169}Tm. Griffith[16] has shown that for a non-Kramers ion $g_\perp \equiv 0$ and only $\Delta^2 = \Delta_x^2 + \Delta_y^2$ represents an observable; Δ is the zero magnetic field energy separation between levels 1 and 2.

The eigenvalues for Eq. (1) are given as

$$\hbar\omega = \pm\tfrac{1}{2}[(g_\parallel \mu_B H_z + A_\parallel I_z)^2 + (\Delta_x + G_\perp \mu_B E_x)^2 + (\Delta_y + G_\perp \mu_B E_y)^2]^{1/2} . \quad (2)$$

Neglecting $G_\perp$ this result is identical to that obtained for magnetic dipole transitions alone using the quasidegenerate perturbation theory reported earlier.[1,17]

B. Orientation-dependence measurements

Examples of observed spectra of the hydrated chloride and sulfate salts have been reported earlier.[1] The present study has extended earlier work by measuring the observed resonances as a function of angle between the $g_\parallel \cos\alpha$ direction and the external magnetic field.

Figure 1 for the hydrated chloride shows the orientation dependence of each observed hyperfine resonance. The spectrum was recorded at 1.5°K using the K_a band spectrometer. To analyze the angular dependence, we determined the average magnetic field at a given orientation using $H_{av} = \frac{1}{2}(H_1 + H_2)$, where H_1 and H_2 represent the high- and low-field hyperfine lines, respectively.

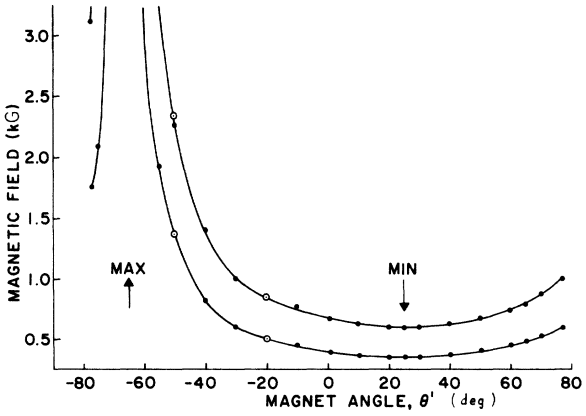

FIG. 1. Orientation dependence of resonance observed in 0.5% Tm^{3+} in $YCl_3 \cdot 6H_2O$ at 1.5°K for sample in $H_\parallel$ at 34.67 GHz. Angle MIN is the angle at which the H (external magnetic field) direction is nearly parallel to $\vec{\mu}$ of the crystal and angle MAX is the angle at which H is perpendicular to $\vec{\mu}$.

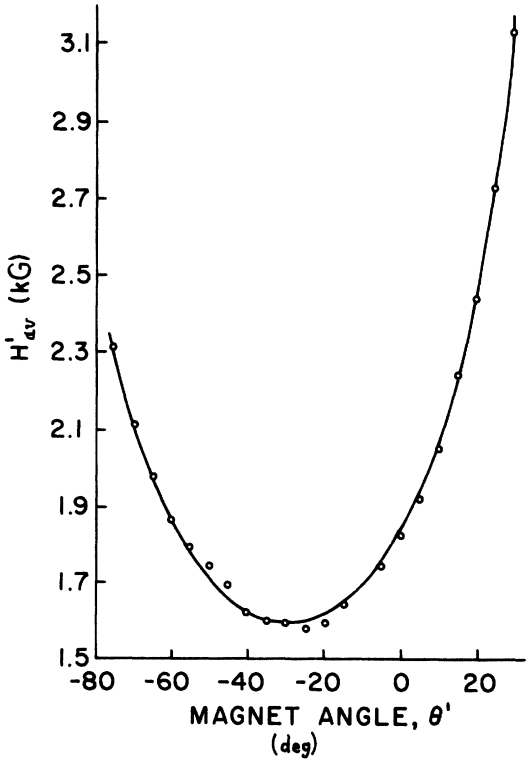

FIG. 2. Average magnetic field H'_{av} (kG) of the two hyperfine-split resonances vs magnet angle θ' for 0.5% Tm^{3+} in $YCl_3 \cdot 6H_2O$ at 1.5 °K and at 35.1 GHz with sample in $H_{\|}$. Data points are connected by a curve whose parameters $A = 1602$ G/cm^{-1} and $B = -29.0°$ were established from a NLLS analysis; $\sigma = 14.6$ G and $R = 0.006$.

This approach is reasonable when the hyperfine interaction is small. Since the frequency was varied slightly throughout the experiment, to obtain as complete an angular dependence as possible, we corrected H_{av} through the following expression:

$$H'_{av} = \frac{H_{av}}{(h^2\nu^2 - \Delta^2)^{1/2}} = \frac{A}{\cos(B - \theta')}, \qquad (3)$$

which comes from Eq. (2) ignoring the hyperfine interaction and ignoring the $G_\perp$ terms.

In Fig. 2 we plot H'_{av} versus magnet angle θ'. The data points are connected by a smooth curve based on Eq. (3) where parameters A (1602.0 G/cm^{-1}) and B (−29.0°) have been determined from a nonlinear least-squares (NLLS) analysis; A represents the minimum value of H'_{av} and B is the angle at which the minimum occurs. The data appearing in Figs. 1 and 2 come from different experiments carried out at slightly different orientations and at slightly different frequencies. Thus the value of B (minimum angle) in Fig. 1 is not the same as B associated with Fig. 2. For the curve in Fig. 2 the standard deviation σ is 14.6G and

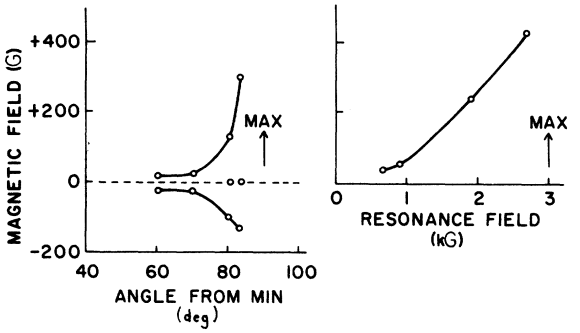

FIG. 3. Splitting (in gauss) of the low-field hyperfine resonance into two components with a third resonance appearing as magnet angle approaches a direction where $\vec{\mu}$ of the crystal is perpendicular to H (external magnetic field). High-field resonances shows similar behavior. Hydrated chloride data recorded at 1.5 °K and 34.5 GHz with sample in $E_\perp$.

the residual R is 0.006. We see that the orientation dependence of the data follows rather well the reciprocal cosine relation given in Eq. (3).

As the angle between $g_{\|}\cos\alpha$ and the external magnetic field approaches 90°, each of the observed hyperfine resonances splits into two with a third resonance appearing between the two. Figure 3 shows data points of the low-field resonance as the angle from the minimum is increased. The higher-field resonance shows the same splitting. We do not have an explanation for these observations. However, the center of gravity of these splittings does produce a mean value of H'_{av} that

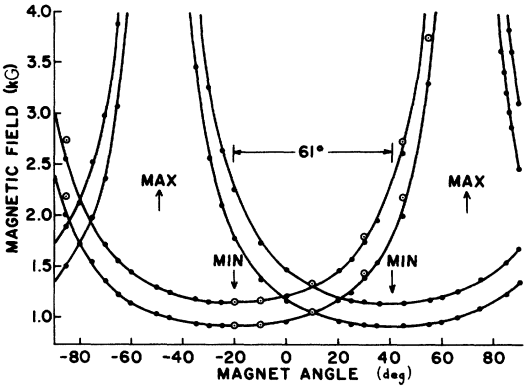

FIG. 4. Orientation dependence of resonances observed in 0.5% Tm^{3+} in $Y_2(SO_4)_3 \cdot 8H_2O$. Sample positioned so that plane containing the two magnetic moments is parallel to plane of rotation of H (external magnetic field). MIN refers to angle at which H and $\vec{\mu}$ are nearly parallel for a given site; MAX refers to angle at which $\vec{\mu}$ is perpendicular to H. Data recorded at 1.6 °K and 24.7 GHz with sample in $E_\perp$.

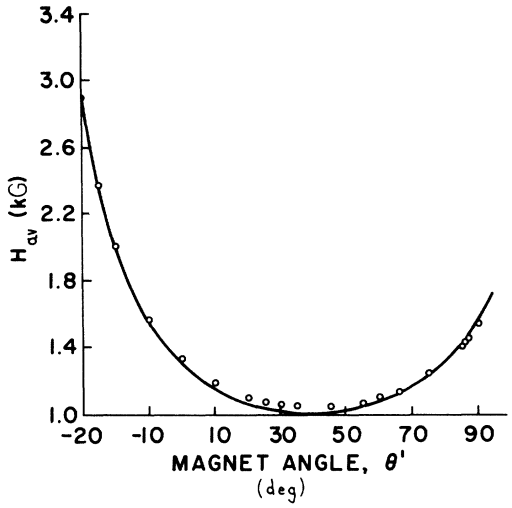

FIG. 5. Average magnetic field H_{av} (kG), of the two hyperfine-split resonances vs magnet angle θ' for one site of 0.5% Tm^{3+} in $Y_2(SO_4)_3 \cdot 8H_2O$ at 1.6 °K and at 24.7 GHz with sample in $E_\perp$. Data points are connected by a curve whose parameters $A = 1002$ G and $B = -40.1°$ were established from a NLLS analysis; $\sigma = 26.9$ G and $R = 0.016$.

lies on the curve shown in Fig. 2.

Figure 4 shows the orientation dependence of the resonances seen in the hydrated sulfate salts. As pointed out earlier,[1,11] two types of sites have been observed at an angle of approximately 60° to one another. From the present K_a-band data we have obtained an average value of 60.4° representing the angle between the two magnetic moment

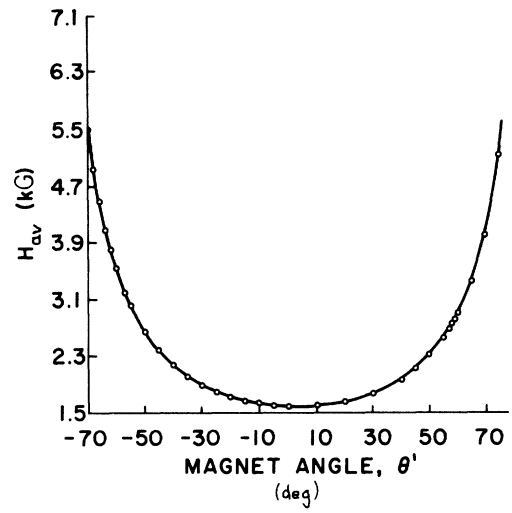

FIG. 6. Average magnetic field H_{av} (kG), of the same two hyperfine-split resonances vs magnet angle θ' as described in Fig. 5, except taken at 1.5 °K and 34.6 GHz with sample in $E_\perp$; $A = 1590$ G, $B = +3.1°$, $\sigma = 15.0$ G, and $R = 0.004$.

directions. From the K-band data we have obtained an average value of 60.6°. The spectra in Fig. 4 taken at 1.6°K using the K-band spectrometer involve the sample positioned so that the $g_{\parallel}$ directions for the two sites form a plane that is nearly parallel to the plane of rotation of the external magnetic field. At any given orientation the intensities of the resonances for each site are nearly the same indicating a nearly equal abundance of both sites. The reported intensities of Zeeman-split absorption lines are also found to be nearly equal for both sites.[11]

Figures 5 and 6 show the orientation dependence of the average of the two hyperfine resonances, H_{av}, associated with one of the sites. The pattern is the same for the second site except it is shifted by approximately 60° from the first. In Fig. 5 the data were taken at 1.6 °K using the K-band spectrometer. In Fig. 6 the data were taken at 1.5°K using the K_a-band spectrometer. A NLLS analysis was made on data associated with each site and at the two different frequencies. The resulting curves obtained from such an analysis appear in Figs. 5 and 6. The standard deviation σ and the residual R are larger for data collected at the lower frequency. At the higher frequency (Fig. 6) σ and R are slightly smaller than found for the hydrated chloride data given in Fig. 2. At both frequencies we see the reciprocal cosine relation given in Eq. (3) as describing the orientation dependence of the data.

As the angle between $g_{\parallel}\cos\alpha$ and the external magnetic field is increased, we observe a splitting of the hyperfine lines for each site. In addition to this splitting a pair of weak satellite resonances observed even at the minimum angle begins to shift rapidly away from the center of gravity as shown in Fig. 7. Presently, we can only speculate on one or more possible explanations. We need to know the crystal structure in greater detail, and we need to carry out further experiments involving different concentrations of Tm^{3+}.[17-20]

From the data presented so far it is possible to establish values of $g_{\parallel}\cos\alpha$ and Δ. Rewriting Eq. (3) in terms of frequency ν, we obtain

$$\nu^2 = (1/h^2)[(g_{\parallel}\cos\alpha)^2\mu_B^2 H_{av}^2 + \Delta^2]. \quad (4)$$

If we plot ν^2 vs H_{av}^2, we obtain a straight line whose slope is $(\mu_B g_{\parallel}\cos\alpha)^2/h^2$ and whose intercept is Δ^2/h^2. In Table I we present the results of the present study together with results from an error analysis of $g_{\parallel}\cos\alpha$ and Δ for data reported earlier.[1,3,7,11] The details of the error analysis are described by one of us[13] (I. E. R.). In addition to presenting our results, Table I serves a useful purpose in bringing together the same parameters deduced from different experiments and from theo-

TABLE I. Summary of results obtained for Tm^{3+} in hydrated chloride and sulfate crystals.

Crystal	T (°K)	$g_{\parallel}\cos\alpha$	Δ (cm^{-1})	$A_{\parallel}/\cos\alpha$ (G)	Method and Ref.
Tm^{3+} in $YCl_3 \cdot 6H_2O$		13.7	"Almost degenerate" (Ref. 3)		CEF calculation (Ref. 3)
0.5% Tm^{3+} in $YCl_3 \cdot 6H_2O$	4.2	14.00 ± 0.05	1.12 ± 0.01	243 (33.7–36 GHz)	Microwave resonance (Ref. 1)
		14.05 ± 0.36	1.117 ± 0.006		Present analysis of raw data in Ref. 1
2% Tm^{3+} in $YCl_3 \cdot 6H_2O$	77	13.5	1.3 ± 0.3		Optical Zeeman data (Ref. 2)
$TmCl_3 \cdot 6H_2O$	4.2	13.91	0.3		CEF calculation (C_2sym.) (Ref. 4)
		14.00	0.4		CEF calculation (D_6sym.) (Ref. 5)
0.5% Tm^{3+} in $YCl_3 \cdot 6H_2O$	1.5	13.37 ± 1.08	1.12 (Ref. 1)	246 ± 2 (24.7 GHz)	Present study
0.5% Tm^{3+} in $Y_2(SO_4)_3 \cdot 8H_2O$	4.2	13.4	0.61 ± 0.02	243 (33.7–36 GHz)	Microwave resonance (Ref. 1)
		13.4 ± 1.83	0.61 ± 0.21		Present analysis of raw data in Ref. 1
$Tm_2(SO_4)_3 \cdot 8H_2O$	77	14.2	0.64 ± 0.1		Optical Zeeman data (Ref. 11)
	4.2	13.9	1.2		CEF calculation (C_{1h}sym.) (Ref. 7)
	4.2	14.00	0.4		CEF calculation (C_{6v}sym.) (Ref. 8)
0.5% Tm^{3+} in $Y_2(SO_4)_3 \cdot 8H_2O$	1.5 – 1.6	14.16 ± 0.19	0.49 ± 0.04	225 ± 4 (24.7 GHz) 241 ± 4 (35.6 GHz)	Present study

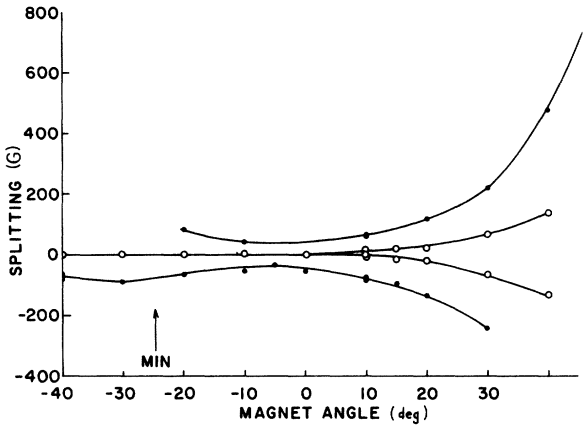

FIG. 7. Splitting (in gauss) of high-field hyperfine resonance of one site of 0.5% Tm^{3+} in $Y_2(SO_4)_3 \cdot 8H_2O$ into two components (inner pair on right-hand side of graph). Weaker satellite lines (outer pair on right-hand side of graph) separate more rapidly as the angle between a given $\vec{\mu}$ and H increase toward 90°. Data recorded at 1.5 °K, 34.9 GHz with sample in $E_{\perp}$. Low-field hyperfine resonance and resonances from other site show similar behavior.

ry.

In columns 3 and 4 in Table I the limits of uncertainty arise when $g_{\parallel}\cos\alpha$ and Δ are determined from Eqs. (3) and (4), where the results depend on a very small difference between two large numbers. Even though the large numbers involve such terms as the magnetic field and the microwave frequency, which are known to better than 1%, the uncertainty associated with the very small difference is calculated to be much larger as Table I shows. $A_{\parallel}/\cos\alpha$ is determined using the separation between hyperfine lines at the angle where the magnetic field is a minimum. In Table I the microwave resonance experimental values reported are for ED transitions. We observed that both ED and MD resonances occurred at the same field value to within experimental error.

The present study reports a different value of Δ for the hydrated sulfate than that reported earlier.[1] The new value is based on having a greater frequency range that allows us in Fig. 8 to obtain a better value of the intercept which is a measure of the separation between the two Stark levels in zero magnetic field. Additional frequency depen-

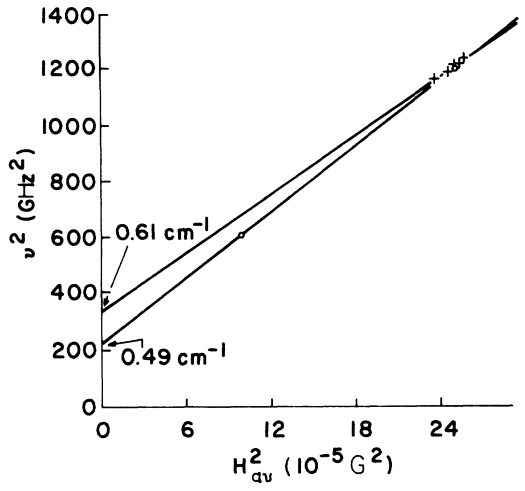

FIG. 8. Determination of Δ at zero magnetic field for 0.5% Tm^{3+} in $Y_2(SO_4)_3 \cdot 8H_2O$. Data include frequency dependence values, O, from present work and values, X, from Ref. 1. Upper extrapolated straight line is based on Ref. 1 only; lower extrapolated straight line includes present K-band data which would indicate a straight line extrapolation to 0.49 cm^{-1} rather than 0.61 cm^{-1} reported in Ref. 1. All values reported for this study were taken at T °K between 1.5 and 1.6 °K with sample in $E_\perp$.

dence studies will help to diminish the uncertainty in establishing Δ. The present values of $A_\parallel/\cos\alpha$ agree with earlier work with the exception that the value obtained for the hydrated sulfate salt using the K-band spectrometer has a smaller value than values obtained using the K_a-band spectrometer. We have no explanation for this apparent frequency dependence.

C. Relative-intensity measurements

We have observed both ED and MD microwave transitions in both salts. Both types of transitions have intensities comparable to the intensity of the 10^{16} spin 2,2-diphenyl-1-picrylhydrazyl (DPPH) sample used as a standard along with the crystals. The relative intensities of the hydrated chloride resonances were studied more completely since these crystals exhibited the simpler spectra of the two different salts. To obtain the ratio I(ED)/I(MD), the sample was placed in two different positions in the cavity as described earlier. A separate run was required for the crystal in each position. However, the DPPH sample was kept at the same position in the cavity for each run so that we could compensate for changes in the microwave power from one run to the next. Every effort was made to maintain a constant temperature of 1.6 ± 0.1°K for both runs. The angular dependence of the intensities was qualitatively the same for both types of transitions. Within the uncertainties associated with these measurements we found for the hydrated chloride crystals $I(\mathrm{ED})/I(\mathrm{MD}) = 1.16 \pm 0.23$.

Knowing this ratio it is possible to determine the parameter $G_\perp$ associated with ED transitions. From Ref. 13, following a lengthy derivation, based on earlier work of Wolf and Jeffries,[21] we have obtained the following expression:

$$G_\perp^2 = \left(\frac{I(\mathrm{ED})}{I(\mathrm{MD})}\right) \frac{(g_\parallel \epsilon)^2(\Delta/\hbar\omega)^2}{(D_\perp/H_\parallel)^2[1-(\Delta/\hbar\omega)^2]}, \tag{5}$$

where T°K and $\hbar\omega$ are assumed constant for the two runs, ϵ is the dielectric constant for the salt,[22] and $D_\perp/H_\parallel$ represents the ratio of the maximum microwave electric to microwave magnetic fields in the sample cavity. For dielectrics the electric field in the sample is related to the electric field in the cavity by $D_\perp = \epsilon E_\perp$ so that $\epsilon^2/(D_\perp/H_\parallel)^2 = 1/(E_\perp/H_\parallel)^2$. Using the field equations given by Poole,[23] we can calculate this ratio which agrees with the value used by Wolfe and Jeffries,[21] namely $(E_\perp/H_\parallel)^2 = 0.25 \pm 0.1$. Using values of $g_\parallel = 14$, $\Delta = 1.12$ cm^{-1}, and $\hbar\omega = 1.154$ cm^{-1}(34.6 GHz), we obtain for the hydrated chloride samples

$$|G_\perp| = 115 \pm 35 \text{ cgs units.} \tag{6}$$

This large value suggests we determine the static $E_\perp$ field needed to induce a resonance. Equation (2) can be rewritten using perpendicular components rather than reference to x and y directions. Neglecting hyperfine structure and letting $H_z = 0$, we obtain

$$G_\perp \mu_B E_\perp = h\nu - \Delta, \tag{7}$$

which gives us a value of $(2.1 \pm 0.6) \times 10^3$ V/cm for $E_\perp$ in the sample. To obtain the applied (external) electric field needed to induce ED transitions we multiply $E_\perp$ by the dielectric constant which is taken to be[22] 8 ± 1.6 and obtain $D_\perp = (1.7 \pm 0.2) \times 10^4$ V/cm. It is feasible to obtain such fields in a TE_{011} cavity which can be made about 1 cm long at 35 GHz.

It is interesting to compare our value of $|G_\perp|$ with values obtained by others who studied different rare-earth ions diluted into different crystals.[15,18,21] Williams[18] obtained $|G_\perp| > 1.5$, $g_\parallel = 2.5$ cgs units for non-Kramers $Pr^{3+}(4f^2)$ doped into yttrium ethylsulfate. For the same ion diluted into La-Zn double nitrate Culvahouse *et al.*[15] obtained $|G_\perp| = 2.6$ cgs units. For the Kramers ion Yb^{3+} doped into yttrium ethylsulfate Wolf and Jeffries[21] obtained 0.4 cgs units for $|G_\perp|$. Efforts have been made by all these authors to calculate $|G_\perp|$ using theoretical models. The much larger value for $G_\perp$ reported here is due to the large ex-

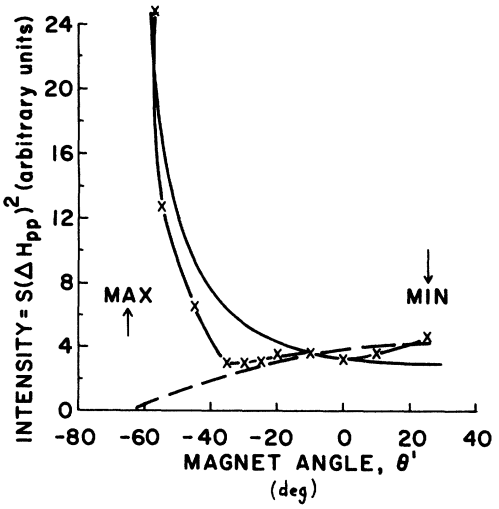

FIG. 9. Orientation dependence of the average intensity of the two hyperfine resonances of 0.5% Tm^{3+} in $YCl_3 \cdot 6H_2O$. MAX and MIN are defined in Fig. 1, for example. Dashed line is predicted $[\cos(25°-\theta')]$ dependence; solid line is a $[\cos(25°-\theta')]^{-1}$ dependence. Data recorded at 1.5 °K and 34.7 GHz with sample in $H_{\|}$. Data points are given as X's.

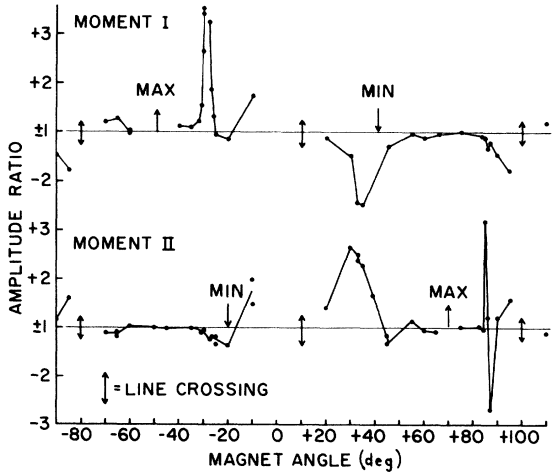

FIG. 10. First-derivative amplitude ratio versus magnet angle for observed resonances of either site in 0.5% Tm^{3+} in $Y_2(SO_4)_3 \cdot 8H_2O$ at 1.6 °K, 24.7 GHz, and with sample in $H_{\|}$. MAX and MIN defined in Fig. 1, for example. The ratio is positive when low-field hyperfine-split resonance is larger and negative when the high-field resonance is larger.

perimental values for $g_{\|}\cos\alpha$ and Δ.

In Fig. 9 we give an example of the variation of relative intensity with angle for the hydrated chloride. The data were taken at 1.5 ± 0.1°K using the K_a-band spectrometer with the sample in $H_{\|}$. The intensity of the resonances were taken as proportional to the peak-to-peak amplitude S times the peak-to-peak linewidth ΔH_{pp} squared. The average of the measured intensity of the two hyperfine lines is given in Fig. 9. The intensity measurements were not easy to make over the entire orientation angle so that the error associated with certain data points can be large.

In Ref. 13 the intensity for ED and MD microwave transitions was calculated for Tm^{3+} in the hydrated chloride and sulfate salts. These calculations showed that both I(ED) and I(MD) were directly proportional to a $\cos\theta$ angular dependence neglecting hyperfine interaction. In Fig. 9 we show as dashed lines the predicted angular dependence of the intensity when the sample is in position to observe MD transitions. Between −40 and +25 deg of magnet angle θ' the intensity data appear to follow the $(\cos\theta)$ dependence predicted in Ref. 13.

However, at larger angles from the $g_{\|}\cos\alpha$ direction where the two hyperfine lines are observed to split, the intensity changes direction and increases rapidly like a $(\cos\theta)^{-1}$ dependence rather than the predicted $(\cos\theta)$ dependence. This effect probably results from the fact that each hyperfine line splits into several components at these larger angles, thus making the linewidth appear much broader, causing the intensity, which goes as the peak-to-peak linewidth squared, to increase rather than decrease as expected at the larger angles. The mechanism(s) causing the splitting need to be explored before we can interpret the intensities at the larger angles. In Fig. 9 a $(\cos\theta)^{-1}$ dependence is also plotted for comparison. Within experimental uncertainties it is possible that a $(\cos\theta)^{-1}$ dependence may be found over the entire range of angles observed.

We have also examined the relative peak-to-peak amplitudes of the hyperfine lines as a function of angle for the hydrated sulfate crystals at 24 and 35 GHz. Figure 10 shows a plot of our results at 24 GHz taken at 1.6°K. On the graph MIN refers to the $g_{\|}\cos\alpha$ direction and MAX refers to 90° from that direction. The convention in assigning the amplitude ratio signs is as follows: If the low-field line peak-to-peak amplitude was greater than the high-field line peak-to-peak amplitude, the sign was assigned a positive value. Two different effects can be seen in Fig. 10. Whenever the lines from one site cross the lines from the other site, the amplitude ratio appears to be affected. This effect may indicate a coupling between the Tm^{+3} in the two sites. The other effect appears around 20° to the right of MAX where we observe a rapid positive excursion of the amplitude ratio for magnetic moment I. This same effect is observed about 17° to the right of MAX for moment II, except that it has a rapid positive rather than negative excur-

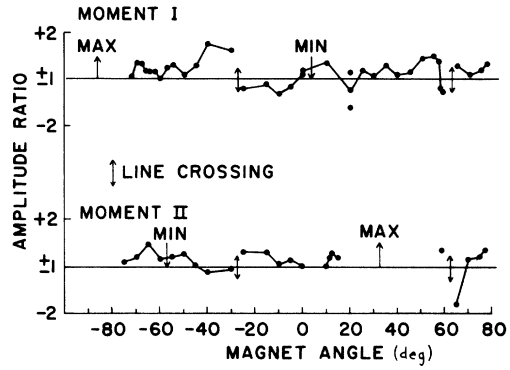

FIG. 11. First-derivative amplitude ratio vs magnet angle for observed resonances of either site in 0.5% Tm^{3+} in $Y_2(SO_4)_3 \cdot 8H_2O$ at 34.6 GHz and 1.5 °K. The ratio is positive when the low-field resonance is larger and negative when the high-field resonance is larger. MAX and MIN are defined in Fig. 1, for example.

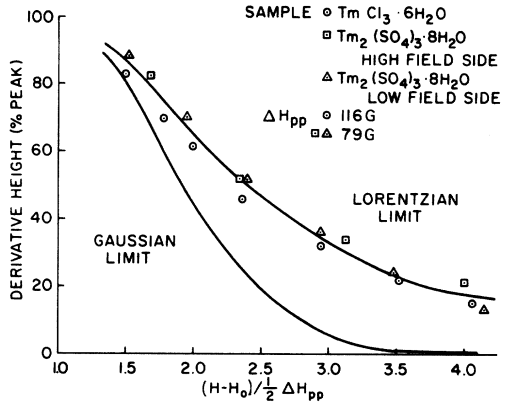

FIG. 12. Resonance line shapes for 0.5% Tm^{3+} in $YCl_3 \cdot 6H_2O$ and $Y_2(SO_4)_3 \cdot 8H_2O$. H_0 is the resonant magnetic field and ΔH_{pp} is the peak-to-peak linewidth. Data recorded at 35.1 GHz, 1.5 °K, and sample in $H_{\|}$.

sion. To see if these effects were frequency dependent, we ran the same sample mounted in the same position at 35 GHz and 1.5°K. These results are shown in Fig. 11. A careful examination for the excursion on moment I did not seem to be present; and, in general, the relative amplitude fluctuations were considerably smaller at 35 GHz. These effects may possibly arise from dipole-dipole coupling or from cross relaxation. We have not seen these effects discussed in any of the literature.

D. Measurement of linewidths and line shapes

We have been able to measure the linewidths of many of the observed resonances at 1.5°K using the K_a-band spectrometer. It is possible to determine the shape of a resonance transition by comparing the percent of derivative heights versus $(H - H_0)/(\Delta H_{pp}/2)$, where H_0 is the center of the line and ΔH_{pp} is the peak-to-peak linewidth, with the calculated Lorentzian and Gaussian limit expressions given in Ref. 13. The lines picked for the analysis of Fig. 12 were chosen because of their high signal-to-noise ratio and consequently were not at a field angle such that $\Delta H_{\|}$ was a minimum. In Fig. 12 the Lorentzian and Gaussian limits are sufficiently different that the data for both salts would indicate the resonances have Lorentzian line shapes. Lorentzian-shaped lines result from time-dependent interactions such as spin-lattice and spin-spin interactions. The fact that the lines are nearly Lorentzian also indicates that Δ more likely arises because of the low-symmetry CEF than from random strains in the crystals. We should point out that at large angles where the resonances are seen to split, the linewidths and line shapes become difficult to establish experimentally.

Figure 13 shows the angular dependence of the measured linewidths taken from the hydrated chloride data at 1.5°K using the K_a-band spectrometer. The linewidths follow a $(\cos\theta)^{-1}$ dependence rather well, except at large angles where splitting of the resonances is observed. A $(\cos\theta)^{-1}$ dependence is predicted in Ref. 13 assuming the broadening is primarily due to lifetime broadening. The predicted $(\cos\theta)^{-1}$ curve is also given in Fig. 13.

For similar salts containing non-Kramer's rare-earth ions in low concentrations (such as ours) spin-lattice coupling is found to be quite strong. If we assume our linewidths are primarily governed by this mechanism, we can estimate T_1, the spin-lattice relaxation time, from the expres-

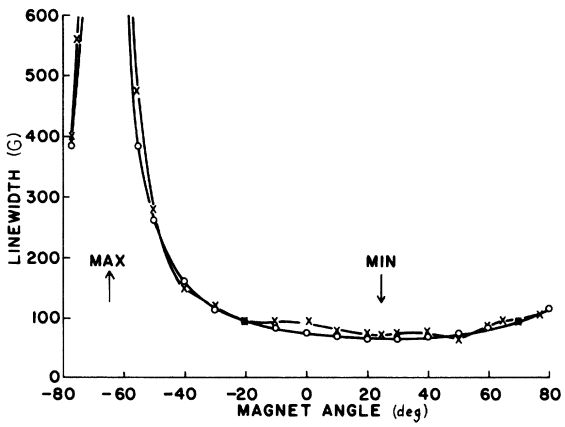

FIG. 13. Average peak-to-peak linewidth of both hyperfine resonances of 0.5% Tm^{3+} in $YCl_3 \cdot 6H_2O$ as a function of magnet angle θ. Data recorded at 1.5 °K, 34.67 GHz with sample in $H_{\|}$. MAX and MIN are defined in Fig. 1, for example.

TABLE II. Average peak-to-peak linewidths and relaxation times.

Sample	Frequency (GHz)	ΔH_{pp} (G) Present microwave data [a]	T_1 (sec)	ΔE (cm^{-1}) (Refs. 17 and 24) Optical data [b]	$\Delta t \geq$ (sec)
0.5% Tm^{3+} in $Y_2(SO_4)_3 \cdot 8H_2O$	34.6	26 ± 5	$(1.9 \pm 0.4) \times 10^{-10}$	(0.14 ± 0.05)	$(3.8 \pm 0.1) \times 10^{-11}$
	24.7	36 ± 5	$(1.3 \pm 0.3) \times 10^{-10}$	(0.14 ± 0.05)	$(3.8 \pm 0.1) \times 10^{-11}$
0.5% Tm^{3+} in $YCl_3 \cdot 6H_2O$	35.1	58 ± 5	$(8.1 \pm 2) \times 10^{-11}$	(0.17 ± 0.05)	$(3.1 \pm 0.1) \times 10^{-11}$

[a] Microwave data reported were taken at 1.5 °K on samples containing Tm^{3+} concentrations listed in first column.
[b] Optical linewidth data measured at half-maximum of linewidth were taken at 4.2 °K of samples containing 2.0% rather than 0.5% Tm^{3+} in the various crystals. The more concentrated crystals were necessary for optical studies since samples were used to establish temperature-dependent Stark levels of the ground-state manifold $^3H_6$.

sion[13]

$$T_1 \approx \sqrt{3} g_{\parallel} \cos\alpha \mu_B \Delta H_{pp}/\hbar . \quad (8)$$

In Table II we present values of T_1 and ΔH_{pp} for the two salts at 1.5°K at K- and K_a-band frequencies. The values of ΔH_{pp} given in Table II are noticeably smaller than those presented in Figs. 12 and 13 because either they were from a run where $g_{\parallel} \cos\alpha$ was not minimized (Fig. 13) or because the measurement was made at an angle that was not the minimum angle for that run (Fig. 12). These values for T_1 appear reasonable when compared with T_1 values given for other rare-earth ions in similar crystals.[14] It is instructive to compare T_1 values in Table II with lifetimes deduced from linewidths observed in the optical spectra of these salts.[17,24] If we conclude that the optical linewidth of an optical transition observed at 4.2°K and 2% dilution factor is due primarily to spin-lattice relaxation between the components of a nearly degenerate ground-state doublet, we can estimate a lifetime for the state using the uncertainty relation $\Delta E \Delta t \geq h$. We note that the T_1 and Δt values are within a factor of 5 of each other. We might also point out that both the higher concentration factor and higher temperature for the optical lines would tend to broaden the optical lines as compared to the EPR lines. If we were to extrapolate the optical results back to the EPR concentration and temperature, the T_1 and Δt values likely would be in even better agreement. Thus, the results in Table II seem to be consistent and imply that the EPR lines and optical lines are homogeneously broadened. A temperature-dependent study of spin-lattice relaxation times seems in order and would shed light on the particular spin-phonon mechanism(s) involved at temperatures between 4.2 and 1.5°K.

ACKNOWLEDGMENTS

We thank Dr. J. E. Bray and Dr. E. R. Lemar, Physics Dept., Washington State University, Pullman, Wa., and Dr. E. A. Karlow, Columbia Union College, Takoma Park, Md., for many helpful discussions and assistance. We also wish to thank Professor R. Willett and Dr. R. Caputo, Chemistry Dept., Washington State University, for crystallographic studies made on the salts described. Dr. Caputo put in many hours in constructing and debugging the automated x-ray diffractometer system which made the structure studies possible.

†All experimental work cited was performed in the Department of Physics at Washington State University, Pullman, Washington 99163. Financial support at WSU came in part under contracts Nos. USAEC AT(45-1)-2221-T6, NSF GU-2631, and in part from NDEA Title IV fellowship funds, and represents part of the Ph.D. dissertation in physics submitted by I. E. Rouse to WSU, 1974.

[1]J. B. Gruber, E. A. Karlow, D. N. Olsen, and U. Ranon, Phys. Rev. B 2, 49 (1970).
[2]D. N. Olsen and J. B. Gruber, J. Chem. Phys. 54, 2077 (1971).
[3]I. H. Harrop, J. Chem. Phys. 42, 4000 (1965).
[4]J. Stöhr, D. N. Olsen, and J. B. Gruber, J. Chem. Phys. 55, 4463 (1971); 60, 1697 (E) (1974).
[5]D. N. Olsen, J. Stöhr, and J. B. Gruber, J. Chem. Phys. 55, 4471 (1971).
[6]J. Stöhr and J. B. Gruber, J. Chem. Phys. 7, 336 (1975).
[7]E. A. Karlow, J. Stöhr, and J. B. Gruber, J. Chem. Phys. 10, 131 (1975).
[8]J. Stöhr, E. R. Seidel, and J. B. Gruber, J. Chem. Phys. 61, 4820 (1974).
[9]M. Marezio, H. A. Plettinger, and W. H. Zachariasen, Acta Crystallogr. 14, 234 (1961).
[10]M. Tinkham, *Group Theory and Quantum Mechanics* (McGraw-Hill, New York, 1964).
[11]E. A. Karlow and J. B. Gruber, J. Chem. Phys. 55, 4730 (1971).

[12]R. S. Alger, *Electron Paramagnetic Resonance: Techniques and Applications* (Interscience, New York, 1968).
[13]I. E. Rouse, Ph.D. thesis (Washington State University, 1974) (unpublished).
[14]A. Abragam and B. Bleaney, *Electron Paramagnetic Resonance of Transition Ions* (Oxford U.P., London, 1970).
[15]J. W. Culvahouse, D. P. Schinke, and D. L. Foster, Phys. Rev. Lett. 18, 117 (1967).
[16]J. S. Griffith, Phys. Rev. 132, 316 (1962).
[17]D. N. Olsen, Ph.D. thesis (Washington State University, 1970) (unpublished).
[18]F. I. B. Williams, Proc. Phys. Soc. Lond. 91, 111 (1967).
[19]D. R. Fitzwater and R. E. Rundle, Unclassified USAEC Document No. 1SC241, TID, Oak Ridge, Tennessee (1952).
[20]V. I. Ivanov, Sov. Phys.-Crystallogr. 9, 553 (1965).
[21]J. P. Wolfe and C. D. Jeffries, Phys. Rev. B 4, 731 (1971).
[22]*Handbook of Chemistry and Physics,* 45th ed., edited by R. C. Weast (Chemical Rubber Company, Cleveland, Ohio, 1964), p. E-33.
[23]C. P. Poole, *Electron Spin Resonance* (Interscience, New York, 1967).
[24]E. A. Karlow and D. N. Olsen (unpublished).